

Fetal Cartilage Progenitor Cells in the Repair of Osteochondral Defects

Bruno C. Menarim, DVM, PhD, Chan Hee Mok, PhD, Kirsten E. Scoggin, PhD, Alexis Gornik, DVM, Emma N. Adam, DVM, PhD, Shavahn C. Loux, PhD, and James N. MacLeod, VMD, PhD

Investigation performed at Gluck Equine Research Center, Department of Veterinary Science, Martin-Gatton College of Agriculture, Food and Environment, University of Kentucky, Lexington, Kentucky

Background: Therapies for cartilage restoration are of great interest, but current options provide limited results. In salamanders, interzone (IZN) tissue can regenerate large joint lesions. The mammalian homolog to this tissue exists during fetal development and exhibits remarkable chondrogenesis *in vitro*. This study analyzed the potential of equine IZN and adjacent anlagen (ANL) cells to regenerate osteochondral defects.

Methods: Osteochondral defects were created in the knee of immunosuppressed rats and were grafted with cell pellets from either equine fetal IZN, equine fetal ANL, adult fibroblasts, or adult chondrocytes, or they were left untreated. Osteochondral repair was assessed after 2, 6, and 16 weeks.

Results: Untreated lesions unexpectedly failed to represent critical-sized defects and at 2 weeks exhibited new subchondral bone covered by a fibrocartilage layer that thinned over time. Fibroblast-treated defects filled with soft fibrous tissue. Chondrocyte-treated repair tissue exhibited strong proteoglycan and COL2 staining but poor integration to the adjacent bone. Defects treated with IZN, ANL, or chondrocyte pellets developed hyaline cartilage with increasing safranin-O and collagen II staining over time. IZN and ANL repair tissues exhibited some evidence of zonal architecture such as native cartilage and the best bone integration; nonetheless, they developed exuberant growth, often causing patellar instability and osteoarthritis.

Conclusions: IZN or ANL cells exhibited some potential to recapitulate developmental features during cartilage repair. However, identifying regulatory determinants of IZN and ANL-derived overgrowths is necessary.

Clinical Relevance: Studies grafting IZN or ANL tissues in larger animal models with regular immune functions may provide additional insights into improving osteochondral regeneration.

Developmental and traumatic orthopaedic injuries often result in cartilage defects. The intrinsic repair of mammalian articular cartilage is limited¹. Hence, the treatment of joint surface lesions is challenging, and the outcome is often osteoarthritis², a prevalent condition associated with the second highest health-care costs in the United States^{3,4}. Developmental cartilage defects are a common finding in horses and represent a substantial toll on the horse industry^{5,6}. Therefore, veterinary and human medicines critically need effective therapies for treating cartilage defects.

Cell therapies for cartilage restoration are of great interest, with microfracture and varying modalities of autologous chondrocyte implantation currently representing the most used

therapies^{1,7}. However, these approaches most commonly result in a neotissue with impaired mechanical properties due to poor integration with the adjacent cartilage and subchondral bone^{1,7}.

During fetal vertebrate limb development, a distinct zone of cells known as the interzone (IZN) initiates synovial joint formation. These flattened layers of cells are located between chondrocytes from the anlagen (ANL) of developing bones⁸. IZN cells are the common progenitors of all synovial tissues but are present only transiently before joint space cavitation⁹. Unlike most vertebrates, axolotl salamanders retain developmental features during adulthood, including non-cavitated distal joints. The persistent IZN enables a remarkable ability to regenerate critical-sized joint lesions⁸. IZN tissue transplanted into critical-

Disclosure: This study was supported by the Morris Animal Foundation and Spy Coast Farm. The Article Processing Charge for open access publication was funded by The Musculoskeletal Research Lab discretionary fund. The **Disclosure of Potential Conflicts of Interest** forms are provided with the online version of the article (<http://links.lww.com/JBJSOA/A731>).

Copyright © 2025 The Authors. Published by The Journal of Bone and Joint Surgery, Incorporated. All rights reserved. This is an open access article distributed under the terms of the [Creative Commons Attribution-Non Commercial-No Derivatives License 4.0](https://creativecommons.org/licenses/by-nc-nd/4.0/) (CCBY-NC-ND), where it is permissible to download and share the work provided it is properly cited. The work cannot be changed in any way or used commercially without permission from the journal.

sized bone defects in axolotls can generate an entirely new diarthrodial joint¹⁰. Cells from the equine IZN and adjacent ANL tissues exhibit remarkable chondrogenesis *in vitro*¹¹. ANL cells exhibit high extracellular matrix (ECM) production comparable with articular chondrocytes, whereas the histological features of IZN cell pellets suggest that they could reproduce the zonal architecture of articular cartilage. These findings suggest that IZN and ANL may serve as cell therapies to repair cartilage defects¹¹. This study assessed the regenerative capacity of equine IZN and ANL cell grafts in repairing critical-sized osteochondral defects and characterized the histology of the resulting tissues. We hypothesized that IZN cell grafts would lead to osteochondral regeneration characterized by hyaline cartilage with zonal structure and subchondral bone integration.

Materials and Methods

Study Design

Thirty-four male rats (16 to 18-week-old, Sprague Dawley Rag2^{-/-} Il2rg^{-/-} (SRG); Hera BioLabs)¹² weighing a mean (and standard deviation) of 349 ± 39 g were housed in a barrier facility, 12:12-hour light:dark cycle, and were used under Institutional Animal Care and Use Committee approval (UKY 2020-3601). The age was selected to ensure skeletal maturity and limit developmental paracrine variables potentially affecting the defect repair response. Animals were acclimated for 1 week before undergoing bilateral knee surgery to create a single os-

teochondral defect in the patellar groove of each hindlimb (Fig. 1). Joints were randomly treated with a graft of equine adult articular chondrocytes (positive control), equine fetal ANL cells, equine fetal IZN cells, equine adult dermal fibroblasts (negative control), or no graft (empty defects, as a negative control). At 2, 6, and 16 weeks after the surgical procedure, the rats were killed, and the joints were dissected and assessed grossly and histologically. Four joints/biological replicates were used per experimental group (graft type) at each time point. Osteochondral sections were subjected to histology (hematoxylin and eosin, safranin-O) and immunohistochemistry (Ki-67 and collagen types I [COL1], II [COL2], and X [COL10]).

Cell Culture and Pellet Preparation

Cell pellets were prepared from primary equine cells archived from previous studies¹¹. Briefly, 4 unsexed equine fetuses (45 to 46 days of gestation) were collected and IZN cells were isolated from between the cuboidal bones of the developing carpus and tarsus through brief enzymatic digestion and recovery of released superficial cells. To isolate ANL chondrocytes, cubes of metaphyseal cartilage from the distal femur and proximal humerus were dissected away from ossification centers and enzymatically digested, and all cells were recovered¹¹. Full-thickness femorotibial articular cartilage shavings and truncal dermal tissue were collected and processed for primary cell isolation from 4 healthy adult male horses killed for reasons unrelated to musculoskeletal disease¹¹.

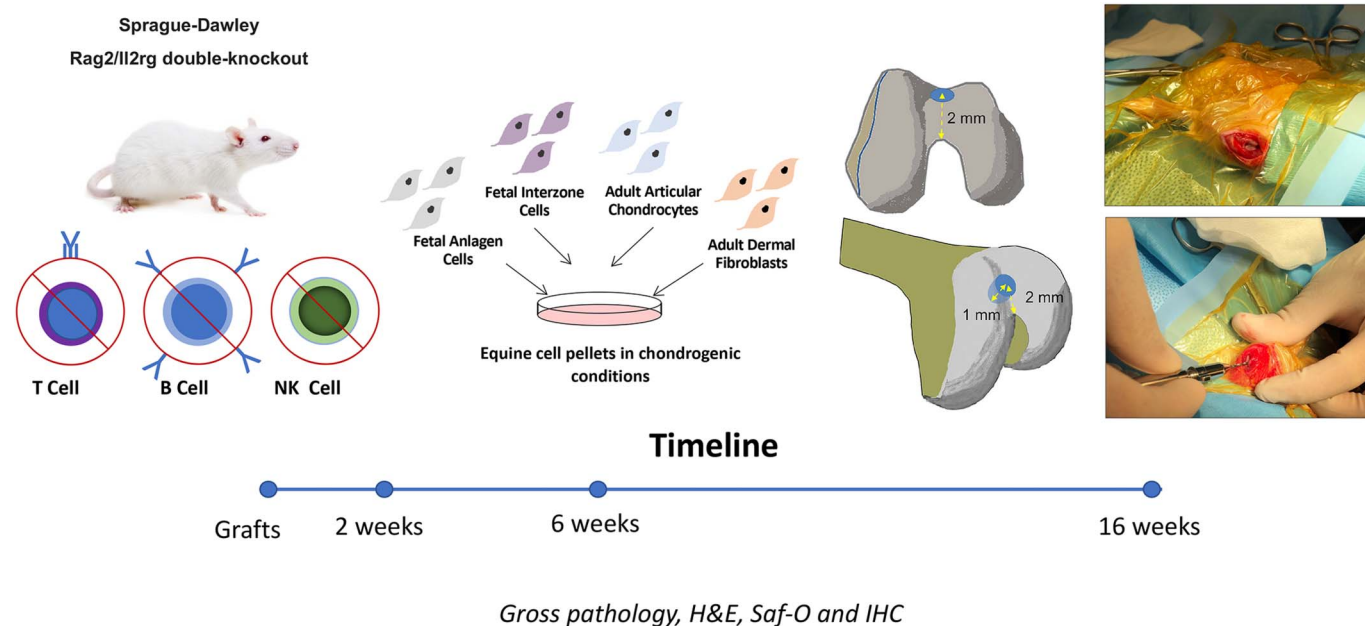


Fig. 1
 Top left: The experimental design, denoting phenotypic and genotypic characteristics of the immunosuppressed rat strain used to host equine cell grafts (upper left) followed by the cell pellet types randomly assigned for treatment of the osteochondral defects. Top middle: Schematic of the anatomical landmarks for creation of the osteochondral defect. (Reprinted from Osteoarthritis Cartilage, Vol. 25, No. 9, Katagiri H, Mendes LF, Luyten FP. Definition of a Critical Size Osteochondral Knee Defect and Its Negative Effect on the Surrounding Articular Cartilage in the Rat. pp. 1531-1540. Copyright 2017, with permission from Elsevier. Open Access Journal.) Top right: Illustration of the surgical field for creation of a single osteochondral defect in each knee (upper right). Bottom: The timeline of the study and the outcome measures assessed at each time point. NK = natural killer, H&E = hematoxylin and eosin, Saf = safranin, and IHC = immunohistochemistry.

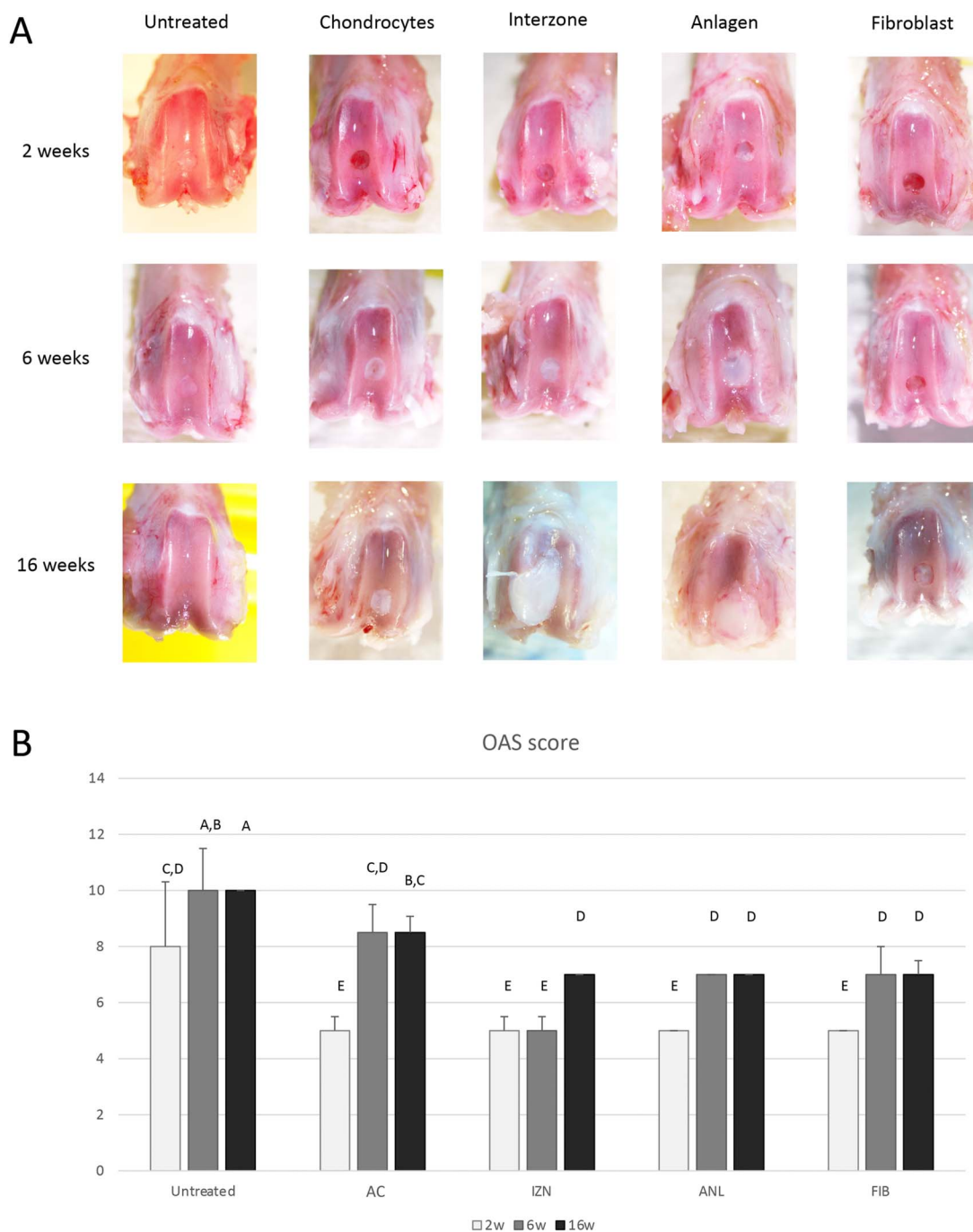


Fig. 2

Fig. 2-A Macroscopic appearance of the repair of osteochondral defects over 16 weeks. Photographs of representative samples show the filling aspect of defects left untreated or treated with adult equine articular chondrocytes (AC) or skin fibroblasts (FIB) or with fetal equine IZN or ANL cells. Untreated defects exhibited the most rapid repair tissue formation and that which most closely resembled normal cartilage. Defects treated with articular chondrocytes produced hyaline cartilage formation levels with visually distinct defect margins. Grafting of fetal cell pellets produced exuberant cartilage tissue overgrowth that was visible earlier in ANL-treated joints but ultimately larger in IZN-treated joints. Defects treated with adult skin fibroblasts behaved as expected, exhibiting loose fibrous tissue at all time points. **Fig. 2-B** Macroscopic assessment of osteochondral repair using the OAS. Data are presented as cumulative scores (mean and standard deviation) and showed superior outcomes for untreated joints. Despite clear macroscopic differences, comparable scores for IZN, ANL, and fibroblast-treated joints reflect limitations of the scoring system criteria. Significantly different groups ($p < 0.05$) are denoted by differing superscripts. In sample groups where all samples had the same score, no error bars are shown.

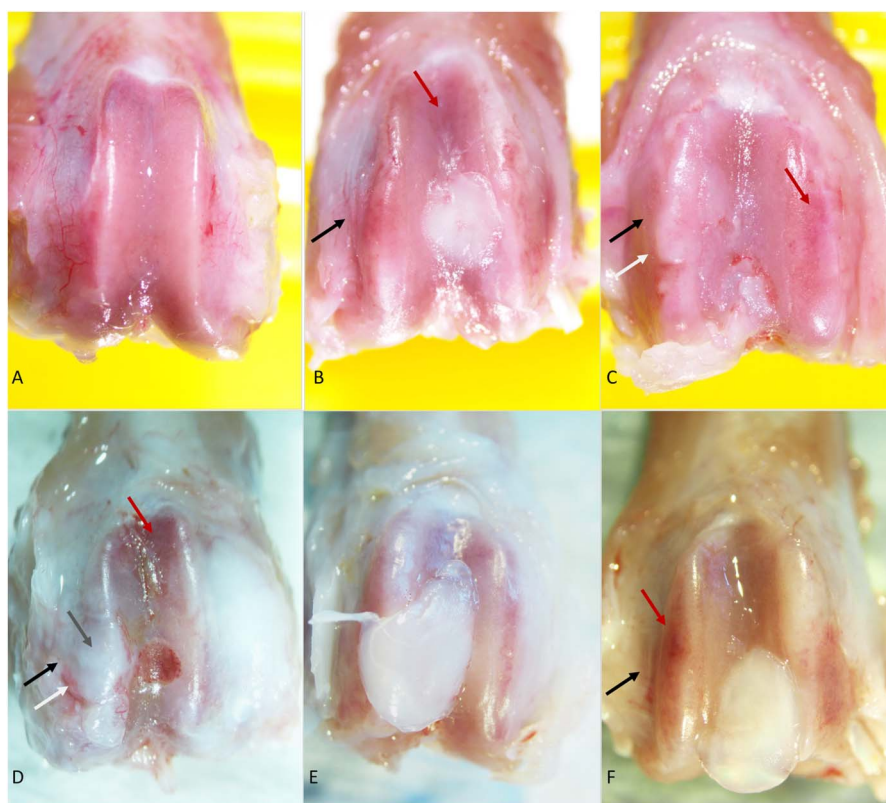


Fig. 3
Gross changes frequently observed in experimental joints. A joint with a healed untreated defect (**Fig. 3-A**) exhibited normal articular surfaces. Another untreated joint (**Fig. 3-D**) exhibited osteoarthritic changes associated with vascularized repair tissue at 6 weeks postoperatively; the contralateral joint of that rat had substantial ANL-derived overgrowth. IZN and ANL-treated joints (**Figs. 3-B, 3-C, 3-E, and 3-F**) exhibited osteoarthritic changes, including trochlear ridge remodeling (black arrows), osteophyte formation (white arrows), fibrous deposition (gray arrow, D), and areas of cartilage thinning (red arrows). ANL-treated joints showed no difference between repair tissue overgrowth from grafting pellets from the same donor with (**Fig. 3-E**) and without (**Fig. 3-F**) chondrogenic induction.

All cell types were cultured in complete medium (Dulbecco's Modified Eagle Medium [DMEM], 10% fetal bovine serum [FBS], 1% penicillin/streptomycin [P/S], 1% amphotericin B) to passage 2, then cryopreserved. For this experiment, passage-2 cells were thawed and cultured to passage 4 in complete medium. Cells were then pelleted by resuspending in complete medium (500,000 cells/mL) and centrifuging 1 mL of the suspension at 500×g for 3 minutes in a 1.5-mL polypropylene microcentrifuge tube. The supernatant was then replaced by chondrogenic medium (high-glucose DMEM, 1% P/S, 12.5-mg/mL bovine serum albumin, 1× Insulin-Transferrin-Selenium-Sodium Pyruvate (ITS-A) supplement, 1× nonessential amino acids, 100-nM dexamethasone, 50-μg/mL ascorbate-2-phosphate, 10-ng/mL recombinant human transforming growth factor β-1 [rhTGFβ1]). After 24 hours of culture at 37°C, and 90% humidity with 5% CO₂, pellets were recovered for grafting¹¹.

Osteochondral Defect Model

Each rat received oral meloxicam (2 mg/kg) preoperatively. The rats were weighed and anesthetized using inhalant anesthesia (1% to 4% isoflurane) under a barrier protocol and received

prophylactic antibiotics (100 mg/kg cefazolin subcutaneously). The rats were prepared for aseptic surgery (2% chlorhexidine scrub followed by 70% isopropyl alcohol, 3 alternated cycles of each) and sterilely draped, with the hindlimbs covered by iodine-impregnated adhesive drapes. Using ophthalmological scalpel blades, a 1-cm skin incision was advanced into the joint capsule adjacent to the medial aspect of the patellar tendon, advancing from its tibial insertion proximally (2 mm) to the insertion of the femoral quadriceps muscle. The patella was laterally displaced, and a single osteochondral defect (2 mm deep × 1.4 mm in diameter) was created in the patellar groove of each distal femur, as previously described¹³, using a murine orthopaedic device (RISystem) (Fig. 1). Using a prior randomization system that ensured that a given treatment was never given bilaterally, defects were filled with 1 IZN or ANL pellet or with 2 pellets of articular chondrocytes or fibroblasts, reflecting differences in pellet sizes between the cell types. No biocompatible glue was used. The patella was repositioned, and the joint capsule and skin were sutured separately (5-0 Monocryl [Ethicon], simple continuous pattern). Rats were recovered and, aside from daily husbandry, were evaluated weekly

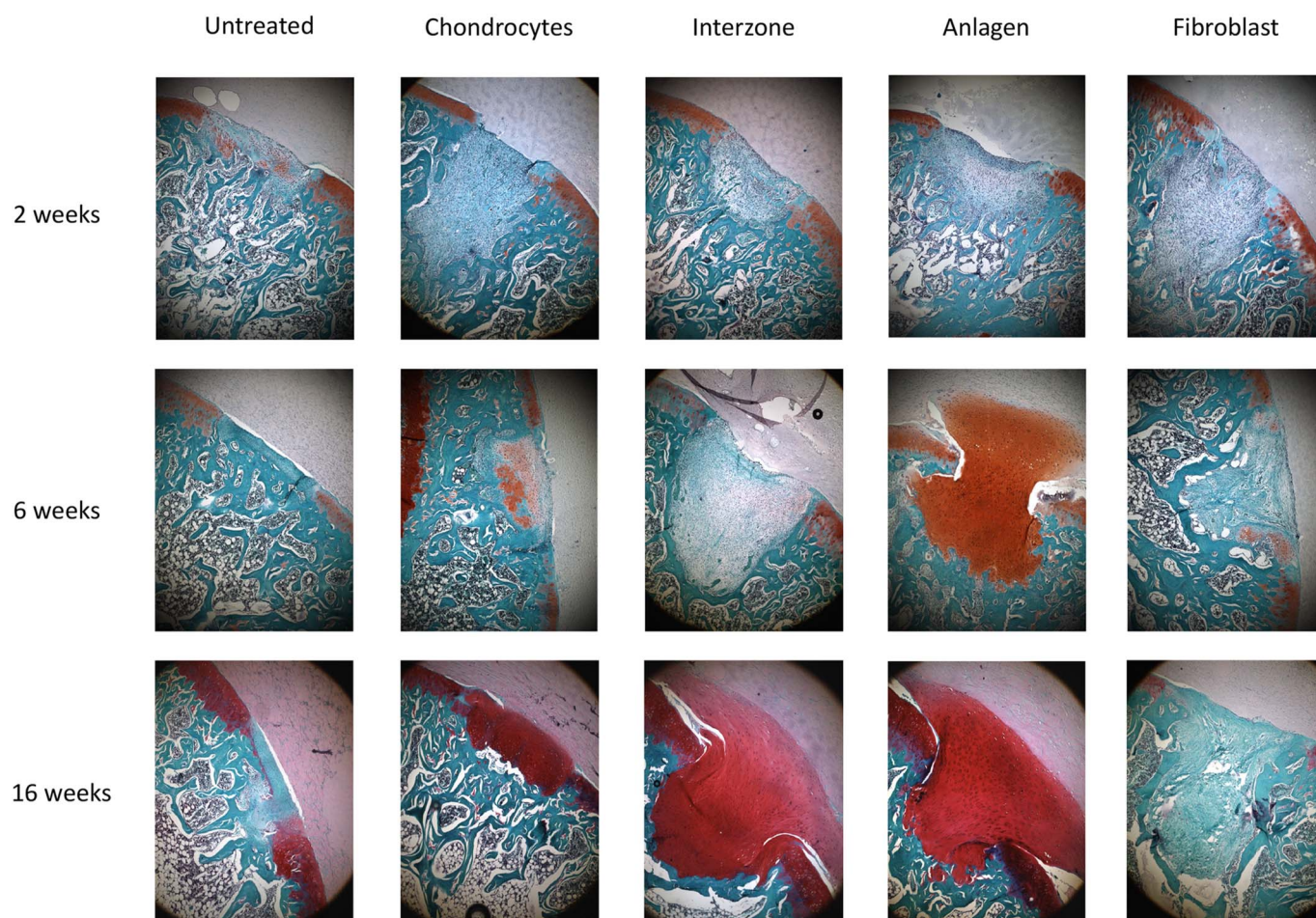


Fig. 4 Photographs of representative samples showing the histologic appearance of the repair of osteochondral defects over 16 weeks. Proteoglycan content is shown by the extent and intensity of safranin-O staining. Untreated defects only exhibited staining at the deeper layer of the repaired tissue. Defects treated with articular chondrocytes exhibited even and intense staining for proteoglycan. Overgrowths from fetal cell pellets exhibited staining for proteoglycan comparable to that of articular chondrocytes, which was seen earlier in ANL-treated joints. Repair tissues from adult skin fibroblasts did not exhibit proteoglycan content at any time point.

for weight, subjective gait assessment, and wound-healing. Meloxicam and cefazolin treatments were repeated at 24 and 48 hours following the surgical procedure. To collect 4 samples for each treatment and time point, 10 rats (with 1 backup for the IZN and ANL treatments) were humanely killed per time point in a CO₂ chamber followed by thoracotomy.

Gross Pathology

Knee joints were dissected, and cartilage repair was grossly assessed. Because scoring systems, including the International Cartilage Regeneration & Joint Preservation Society (ICRS) and O'Driscoll systems, do not account for repair tissue overgrowth¹⁴, the Oswestry Arthroscopic Score (OAS) system was selected because it is also validated for assessing results of cell-based treatments for cartilage repair¹⁵⁻¹⁷. To account for the magnification provided by the arthroscope when applying the OAS system, specimens were evaluated under magnification

(4×, NIKON SMZ1000) and were scored blindly by 3 observers (B.C.M., K.E.S., and A.G.).

Histology and Immunohistochemistry

Following fixation (4% paraformaldehyde) and decalcification (10% ethylenediaminetetraacetic acid [EDTA]), specimens were paraffin-embedded and sectioned (5 to 7 μm). Safranin-O and hematoxylin and eosin staining were performed as previously described¹⁸. For immunohistochemistry, tissue sections were stained using the Polymer-HRP IHC Detection System (QD420-YIKE; BioGenex). For Ki-67 staining, antigen retrieval was performed by incubation with HK087-20K solution (BioGenex) at 95°C for 10 minutes. For COL1, COL2, and COL10, antigen retrieval was performed by pepsin treatment for 10 minutes (R2283; Sigma-Aldrich). The morphology of IZN and ANL overgrown repair tissues prevented applying a histological scoring system for inferential

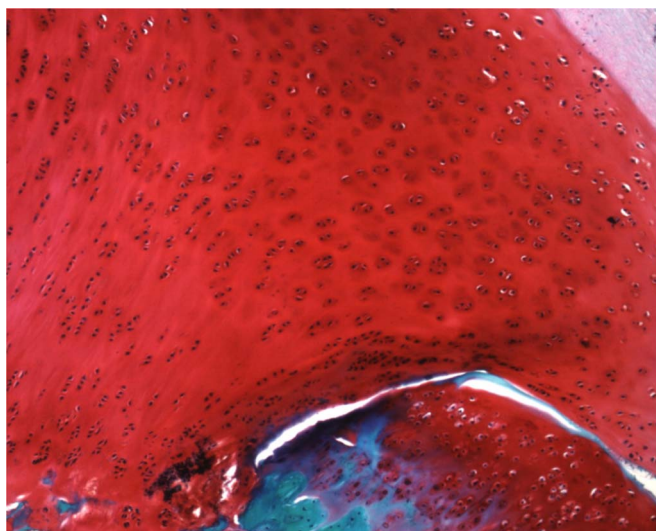


Fig. 5
Representative image of Saf-O stained equine ANL-derived repair tissue demonstrating the morphology and distribution of chondrocytes in a zonal arrangement such as that in native cartilage. Image brightness was adjusted to favor chondrocyte visualization.

statistical analysis, and, thus, our findings are descriptively presented.

Statistical Analysis

Sample size was determined on the basis of the number of available biological replicates of fetal cells from previous *in vitro* studies using aliquots of the same cells^{11,19,20}. Aside from macroscopic assessment, overall data analysis was performed descriptively. Standard least-squares simple linear regression was used to evaluate the differences in OAS between groups, with the model effects of tissue, time, and tissue \times time. Post hoc comparisons were performed using the Student *t* test for Least Square Means (tissue \times time). All statistics were performed using JMP Pro 16.0 (JMP Statistical Discovery), with significance set at $p < 0.05$.

Results

Gross Pathology

Untreated lesions unexpectedly failed to represent critical-sized defects and at 2 weeks exhibited new subchondral bone covered by a fibrocartilage layer that thinned over time (Figs. 2 and 3-A). This was observed by 2 weeks after the surgical procedure in all but 1 lesion. In 1 case, vascularized tissue was observed at 6 weeks (Fig. 3-D). The contralateral joint had substantial ANL-derived overgrowth for that rat, causing joint instability and osteoarthritic changes. The filling of chondrocyte-treated defects was level with adjacent tissues by 6 weeks, but progressively developed a whiter coloration relative to repair tissue from other treatments. Defects treated with fibroblast pellets had filling that was generally below defect edges, but became closer to level by 16 weeks. When probed, fibroblast defects were filled with loose gelatinous tissue that remained softer than the adjacent tissue. Defects treated with IZN or ANL pellets were similar at 2 weeks, displaying trans-

lucent cartilage-like repair tissue level with the defect edges that, over time, became whiter and denser. Unexpectedly, IZN and ANL-treated defects formed an exuberant overgrowth, observed earlier for ANL-treated joints (at 6 weeks) than for IZN-treated joints (at 16 weeks). At 16 weeks, overgrown repair tissue was associated with patellar instability and osteoarthritic changes, including fibrous deposition and remodeling of the femoral trochlear ridge, osteophyte formation, and cartilage thinning (Figs. 3-B, 3-C, and 3-D) in 75% of IZN-grafted joints and 100% of ANL-grafted joints. No osteoarthritic changes were observed in negative or positive control joints. All tissues originating from chondrocyte, IZN, and ANL pellets ultimately exhibited cartilage-like texture and resistance upon probing (Fig. 2-B; see also the Appendix).

To assess whether *in vitro* chondrogenic induction was an important variable contributing to overgrowths in IZN and ANL grafts, 4 additional rats (8 joints) were added to the experiment and were grafted with pellets from the same equine fetal cells without chondrogenic induction. Assessment at 16 weeks postoperatively did not reveal less tissue overgrowth (Figs. 3-E and 3-F).

Histology

Histological changes were consistent with the macroscopic assessments, with untreated joints likewise exhibiting overall superior repair tissue compared with the other treatments (Fig. 4). However, although the repair tissue in untreated joints had a smooth cartilaginous surface that was level with the adjacent cartilage, it was characterized by fibrocartilage exhibiting minimal proteoglycan content, random cell distribution, and varying thickness of subchondral bone advancement. The newly formed subchondral bone had good architecture and integration with the adjacent bone. Satisfactory integration of the repair tissue with native cartilage was observed on at least 1 side of the histological sections. Repair tissue from chondrocyte-treated joints was level with adjacent cartilage, but was often irregular at 6 weeks, at which time moderate proteoglycan content was observed, becoming more marked at 16 weeks. For 2 samples, new subchondral bone developed by 16 weeks, whereas defects in the remaining 2 samples were entirely filled with hyaline cartilage that exhibited poor integration with the adjacent bone. There was no zonal organization of the chondrocytes within the cartilage of chondrocyte-treated samples.

Tissue overgrowth in IZN and ANL-treated joints showed marked proteoglycan staining and was well integrated with the surrounding bone. Cells within the tissue exhibited some zonal stratification similar to native articular cartilage, except lacking a tidemark (Fig. 5). A lacuna-like distribution of smaller chondrocytes was observed in deep layers. Chondrocytes were distributed more evenly in the middle layer and exhibited increasing cytoplasm and proteoglycan staining. The transition from deep to middle zones in repair tissues was usually at the same level as the transition in surrounding recipient tissue. At the outermost layer of IZN and ANL grafts, as in native cartilage, chondrocytes had an even larger amount of cytoplasm with a more flattened horizontal alignment. In ANL-derived tissues, proteoglycan-rich overgrowths were observed and were well integrated with adjacent subchondral

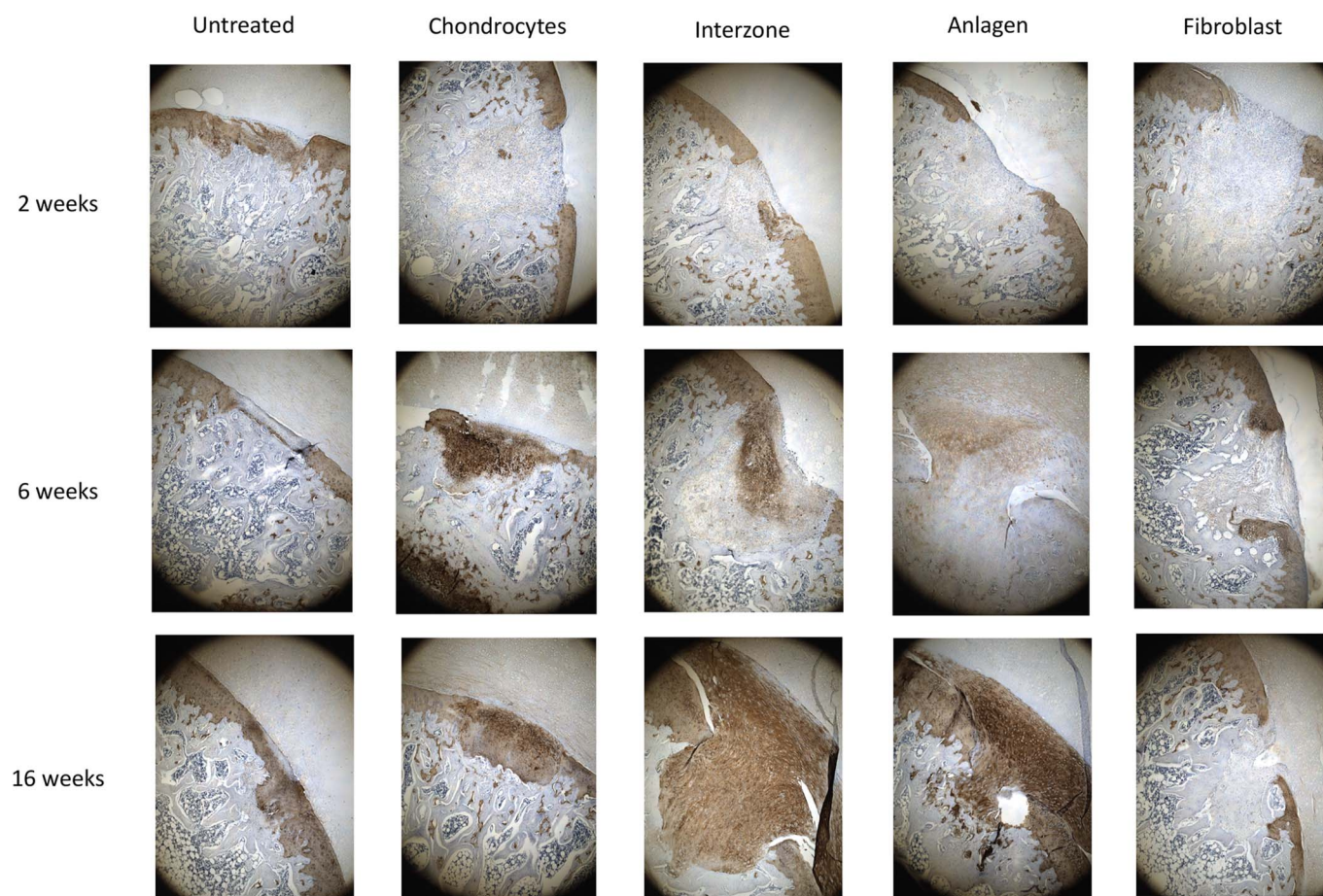


Fig. 6 Immunohistochemistry for COL2 in repair tissues over 16 weeks. COL2 expression was observed in the deeper layers of the repair tissue from untreated defects. Defects treated with articular chondrocytes exhibited even and intense staining. Repair tissues from fetal cell pellets ultimately exhibited comparable intensity of COL2 staining to articular chondrocytes. Repair tissues from adult skin fibroblasts did not exhibit COL2 expression at any time point.

bone by 6 weeks. Such findings were not observed for IZN-treated joints until 16 weeks. Finally, fibroblast-derived grafts exhibited loose fibrous tissue that tended to shrink from its bottom over time and showed no integration or proteoglycan content. In summary, IZN and ANL repair tissues exhibited some evidence of zonal architecture such as native cartilage and the best bone integration; nonetheless, they developed exuberant growth, often causing patellar instability and osteoarthritis.

Immunohistochemistry

Repair tissues were assessed for the proportionate expression of COL2, an indicator of cartilaginous extracellular matrix (Fig. 6); COL1, an indicator of fibrous tissue (Fig. 7); and COL10, an indicator of hypertrophic cartilage (Fig. 8). Although the repair tissue of untreated lesions exhibited varying degrees of COL2 expression, most was localized to deeper layers near the subchondral bone. In contrast, the superficial layer lacked COL2, COL1, or COL10 expression. Like native cartilage, chondrocyte-treated defects expressed abundant COL2, a faint superficial layer coexpressing COL1 and COL10, and mild COL10 expression in the transition to the subchondral bone. IZN and ANL-treated

defects exhibited marked COL2 expression, with a tendency for mild COL1 expression in the osseous attachments and mild to moderate expression of COL1 and COL10 surrounding chondrocytes on the outermost surface of the overgrowths. Fibroblast-treated repair tissues did not express COL2 at any time point, but consistently expressed COL1 and increased COL10 expression over time. Ki-67 expression as an indicator of cell proliferation was not detected in any samples.

Discussion

In this first-of-its-kind study, IZN and ANL cell grafts formed hyaline cartilage with patterns of collagen and proteoglycan expression and cellular organization resembling native cartilage. However, further studies are required to determine why IZN and ANL cells produced overgrowths. When exposed to the synovial environment, hypertrophic chondrocytes like those from ANL lose their hypertrophic capacity and transdifferentiate into an articular phenotype²¹. IZN and ANL cells were culture-passaged, which can lead to epigenetic alterations^{22,23} that often associate with overgrowth and tumorigenesis²³. Our results from Ki-67 staining are not suggestive of cell proliferation and tumorigenesis.

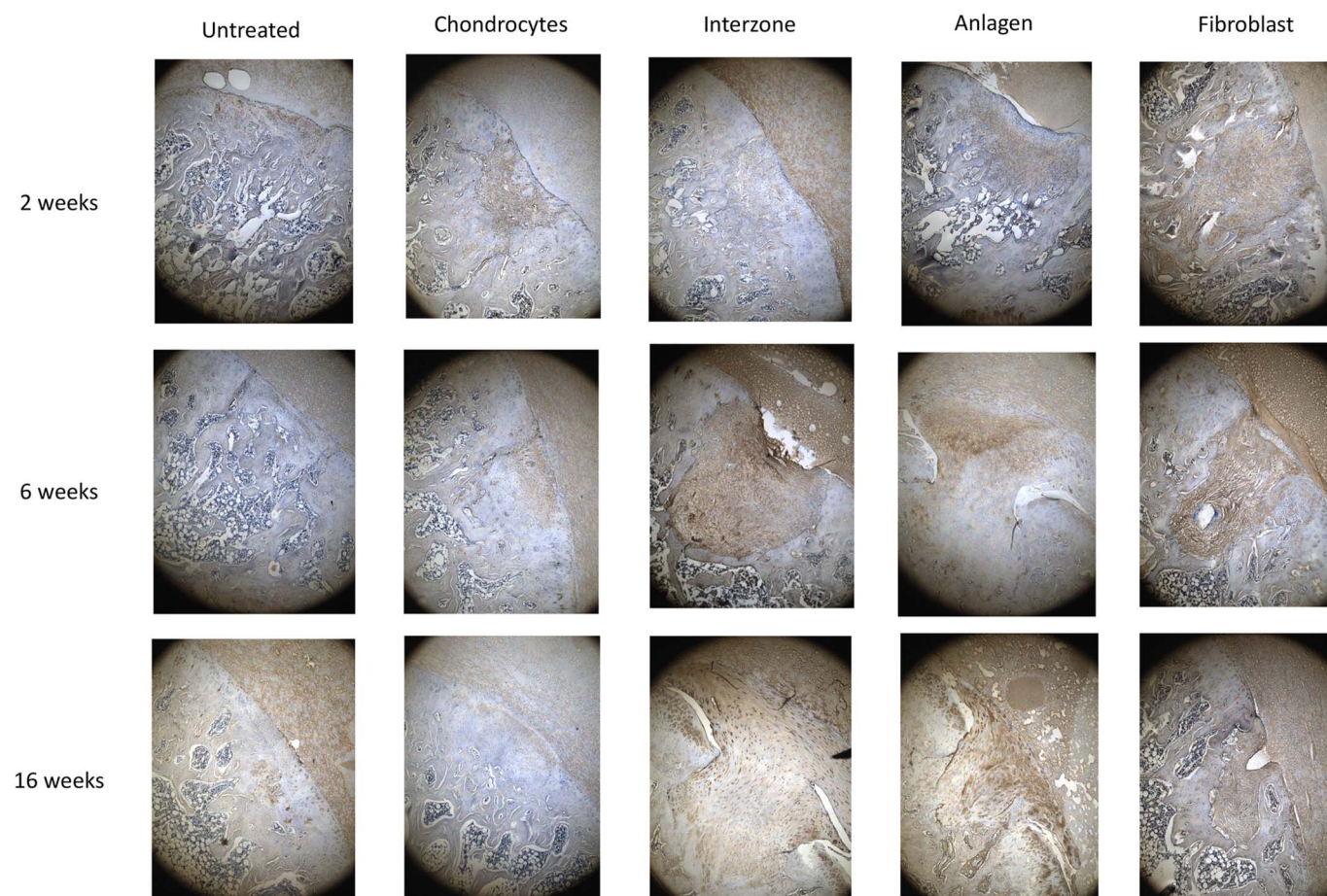


Fig. 7 Immunohistochemistry for COL1 in repair tissues over 16 weeks. Only mild staining for COL1 was observed in the repair tissue from untreated defects at 2 weeks. Repair tissues from chondrocytes exhibited mild COL1 staining closer to its outmost layer. Repair tissues from fetal cell pellets ultimately exhibited moderate COL1 expression, more evident at the outermost layer of ANL-derived tissues. Moderate COL1 expression was consistently observed in repair tissues from adult skin fibroblasts at all time points.

Therefore, graft tissue overgrowth likely results from abundant ECM production. Grafting fewer cells or using IZN or ANL tissue explants instead of culture-expanded cells could potentially address tissue overgrowth.

Zonal stratification resembling native cartilage suggests that IZN and ANL cells have an intrinsic capacity to adjust to mechanical forces, unlike repair tissues from chondrocyte implantation. This could result from superior ECM production and arrangement from IZN and ANL cells relative to chondrocytes²⁴. Although chondrocytes were zonally arranged in IZN and ANL tissues, they displayed a chondron pattern suggestive of overt mechanical stimulation²⁵, which agrees with osteoarthritic changes in the corresponding joints. Expression of distinct collagen types in IZN and ANL tissues also resembled that of native cartilage, with higher COL10 expression in the superficial layers. Conversely, COL1 expression was randomly distributed and higher than in native cartilage. In vitro, after chondrogenic induction, both IZN and ANL express higher COL1 and COL10 than native cartilage^{11,20}.

The successful repair of untreated defects differs from results reported by Katagiri et al., who defined this protocol as providing a critical-sized osteochondral defect model¹³. In our study, untreated defects healed with new subchondral bone as early as 2 weeks after the surgical procedure. This is unlikely to be associated with the severe combined immunodeficiency-like genetic mutation ($Rag2^{-/-} Il2rg^{-/-}$) of SRG rats, as SCID mice have impaired endochondral ossification²⁶, differing from observations in the current study. Differences might be explained by the fact that Cai et al. used the wild-type Lewis rat, whereas we used the Sprague-Dawley rat with the SRG mutation. Lewis and Sprague-Dawley rats have demonstrated differences in tumor necrosis factor-alpha (TNF- α) and interleukin-1 beta (IL-1 β) expression in response to adjuvant-induced arthritis²⁷.

Features from IZN and ANL-derived grafts suggest that repair tissues were of equine origin. Molecular identification of the cells in the graft tissues would strengthen such observation. However, formalin fixation and tissue decalcification limited the range of assays that could be performed. Although each

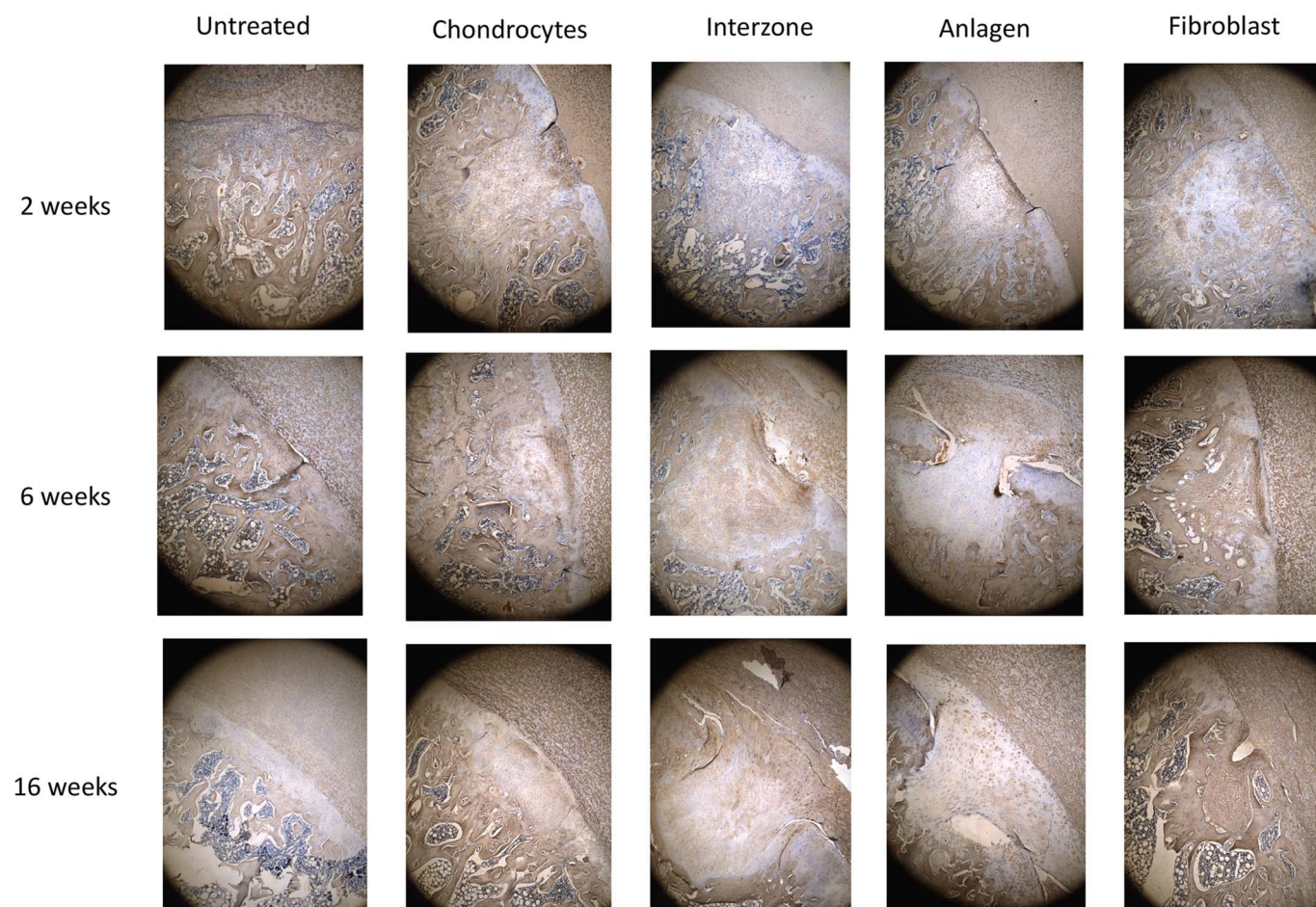


Fig. 8
Immunohistochemistry for COL10 in the repair tissues over the course of 16 weeks. COL10 expression was not observed in the repair tissue from untreated defects. Repair tissues from chondrocytes exhibited mild COL1 staining at the deepest layer and close to its outermost layer. Repair tissues from fetal cell pellets ultimately exhibited moderate-to-marked COL10 expression, more marked in the outermost layer from interzone-derived overgrowths. Marked COL10 expression was consistently observed in repair tissues from adult skin fibroblasts at 6 and 16 weeks.


animal received 2 different treatments, 1 in each hindlimb, there is the potential of systemic cross-talk.

This study had limitations, including the small sample size, its descriptive nature, and the lack of objective gait assessment and indentation modulus measurement. However, the use of an equine osteochondral defect model and major histocompatibility complex-compatible allografts may have overcome limitations of rodent models, such as varying healing capacity of osteochondral defects and the absence of a functional adaptive immune response, known to play a role in tissue repair²⁸.

In conclusion, as previously observed *in vitro*, IZN and ANL cell grafts seemingly recapitulate some developmental features during osteochondral repair *in vivo*, producing hyaline cartilage with a zonal chondrocyte arrangement and ECM content like that of native cartilage. Although such observations represent interesting findings, further studies with larger cohorts are required to overcome the challenges of individual variability and account for the effects of sex differences between graft donors and recipients.

Although there are obvious limits to using fetal cells in humans, recent advances in the successful induction of IZN and ANL-like cells from human-induced pluripotent cells suggest that this barrier can be overcome²⁹. Defining regulatory signaling preventing IZN and ANL overgrowth is also necessary and may further advance the use of fetal-like engineered cells for osteochondral regeneration.

Appendix

 Supporting material provided by the authors is posted with the online version of this article as a data supplement at <http://links.lww.com/JBJSOA/A732>. ■

Bruno C. Menarim, DVM, PhD¹
Chan Hee Mok, PhD²
Kirsten E. Scoggin, PhD¹
Alexis Gornik, DVM³

Emma N. Adam, DVM, PhD¹
Shavahn C. Loux, PhD¹
James N. MacLeod, VMD, PhD¹

¹Gluck Equine Research Center, Department of Veterinary Science, Martin-Gatton College of Agriculture, Food and Environment, University of Kentucky, Lexington, Kentucky

²Department of Orthopedic Surgery, School of Medicine, University of California San Francisco, San Francisco, California

³College of Veterinary Medicine, Lincoln Memorial University, Harrogate, Tennessee

Email for corresponding author: bruno.menarim@uky.edu

References

- Chu CR, Fortier LA, Williams A, Payne KA, McCarrel TM, Bowers ME, Jaramillo D. Minimally manipulated bone marrow concentrate compared with microfracture treatment of full-thickness chondral defects: a one-year study in an equine model. *J Bone Joint Surg Am*. 2018 Jan 17;100(2):138-46.
- McIlwraith C. Traumatic Arthritis and Posttraumatic Osteoarthritis in the Horse. In: McIlwraith CW, Frisbie DD, Kawcak CE, van Weeren PR, editors. *Joint Disease in the Horse*. 2nd ed. St. Louis: Elsevier; 2016. p 33-48.
- Cisternas MG, Murphy L, Sacks JJ, Solomon DH, Pasta DJ, Helmick CG. Alternative methods for defining osteoarthritis and the impact on estimating prevalence in a US population-based survey. *Arthritis Care Res (Hoboken)*. 2016 May;68(5):574-80.
- Torio CM, Moore BJ. National Inpatient Hospital Costs: The Most Expensive Conditions by Payer, 2013: Statistical Brief #204. In: *Healthcare Cost and Utilization Project (HCUP) Statistical Briefs*. Rockville: Agency for Healthcare Research and Quality; 2006.
- Richardson DW. Diagnosis and Management of Osteochondrosis and Osseous Cystlike Lesions. In: Ross MW, Dyson SJ, editors. *Diagnosis and Management of Lameness in the Horse*. 2nd ed. St. Louis: Elsevier Saunders; 2011. p 631-8.
- American Horse Council Foundation. The economic impact of the horse industry on the United States. 2005. Accessed 2024 Sep 25. https://www.eqgroup.com/library/eqstats_us/#:~:text=The%20horse%20industry%20contributes%20approximately,dollars%20for%20the%20U.S.%20economy
- Behrendt P, Feldheim M, Preusse-Prange A, Weikamp JT, Haake M, Eglin D, Rolauffs B, Fay J, Seekamp A, Grodzinsky AJ, Kurz B. Chondrogenic potential of IL-10 in mechanically injured cartilage and cellularized collagen ACI grafts. *Osteoarthritis Cartilage*. 2018 Feb;26(2):264-75.
- Cosden RS, Lattermann C, Romine S, Gao J, Voss SR, MacLeod JN. Intrinsic repair of full-thickness articular cartilage defects in the axolotl salamander. *Osteoarthritis Cartilage*. 2011 Feb;19(2):200-5.
- Jenner F, Ijpma A, Cleary M, Heijnsman D, Narcisi R, van der Spek PJ, Kremer A, van Weeren R, Brama P, van Osch GJ. Differential gene expression of the intermediate and outer interzone layers of developing articular cartilage in murine embryos. *Stem Cells Dev*. 2014 Aug 15;23(16):1883-98.
- Cosden-Decker RS, Bickett MM, Lattermann C, MacLeod JN. Structural and functional analysis of intra-articular interzone tissue in axolotl salamanders. *Osteoarthritis Cartilage*. 2012 Nov;20(11):1347-56.
- Adam EN, Janes J, Lowney R, Lambert J, Thampi P, Stromberg A, MacLeod JN. Chondrogenic differentiation potential of adult and fetal equine cell types. *Vet Surg*. 2019 Apr;48(3):375-87.
- Noto FK, Sangodkar J, Adedeji BT, Moody S, McClain CB, Tong M, Ostertag E, Crawford J, Gao X, Hurst L, O'Connor CM, Hanson EN, Izadmehr S, Tohmé R, Narla J, LeSueur K, Bhattacharya K, Rupani A, Tayeh MK, Innis JW, Galsky MD, Evers BM, DiFeo A, Narla G, Jamling TY. The SRG rat, a Sprague-Dawley Rag2/Il2rg double-knockout validated for human tumor oncology studies. *PLoS One*. 2020 Oct 7;15(10):e0240169.
- Katagiri H, Mendes LF, Luyten FP. Definition of a critical size osteochondral knee defect and its negative effect on the surrounding articular cartilage in the rat. *Osteoarthritis Cartilage*. 2017 Sep;25(9):1531-40.
- Paatela T, Vasara A, Nurmi H, Kautiainen H, Kiviranta I. Assessment of cartilage repair quality with the International Cartilage Repair Society Score and the Oswestry Arthroscopy Score. *J Orthop Res*. 2020 Mar;38(3):555-62.
- van den Borne MPJ, Rajmakers NJH, Vanlauwe J, Victor J, de Jong SN, Bellemans J, Saris DB; International Cartilage Repair Society. International Cartilage Repair Society (ICRS) and Oswestry macroscopic cartilage evaluation scores validated for use in autologous chondrocyte implantation (ACI) and microfracture. *Osteoarthritis Cartilage*. 2007 Dec;15(12):1397-402.
- Goebel L, Orth P, Müller A, Zurakowski D, Bückler A, Cucchiari M, Pape D, Madry H. Experimental scoring systems for macroscopic articular cartilage repair correlate with the MOCART score assessed by a high-field MRI at 9.4 T—comparative evaluation of five macroscopic scoring systems in a large animal cartilage defect model. *Osteoarthritis Cartilage*. 2012 Sep;20(9):1046-55.
- Bonasia DE, Marmotti A, Massa AD, Ferro A, Blonna D, Castoldi F, Rossi R. Intra- and inter-observer reliability of ten major histological scoring systems used for the evaluation of in vivo cartilage repair. *Knee Surg Sports Traumatol Arthrosc*. 2015 Sep;23(9):2484-93.
- Adam EN. Differential gene expression in equine cartilaginous tissues and induced chondrocytes. University of Kentucky; 2016.
- Thampi P, Dubey R, Lowney R, Adam EN, Janse S, Wood CL, MacLeod JN. Effect of skeletal paracrine signals on the proliferation of interzone cells. *Cartilage*. 2021 Dec;13(2_suppl):82S-94S.
- Mok CH, MacLeod JN. Kinetics of Gene Expression Changes in equine fetal interzone and anlagen cells over 14 days of induced chondrogenesis. *Front Vet Sci*. 2021 Aug 9;8:722324.
- Chau M, Dou Z, Baroncelli M, Landman EB, Bendre A, Kanekiyo M, Gkourougianni A, Barnes K, Ottosson L, Nilsson O. The synovial microenvironment suppresses chondrocyte hypertrophy and promotes articular chondrocyte differentiation. *NPJ Regen Med*. 2022 Sep 16;7(1):51.
- Chang-Liu CM, Woloschak GE. Effect of passage number on cellular response to DNA-damaging agents: cell survival and gene expression. *Cancer Lett*. 1997 Feb 26;113(1-2):77-86.
- Blum B, Benvenisty N. The Tumorigenicity of Human Embryonic Stem Cells. *Adv Cancer Res*. 2008;100:133-58.
- Griffin DJ, Bonnevie ED, Lachowsky DJ, Hart JC, Sparks HD, Moran N, Matthews G, Nixon AJ, Cohen I, Bonassar LJ. Mechanical characterization of matrix-induced autologous chondrocyte implantation (MACI®) grafts in an equine model at 53 weeks. *J Biomech*. 2015 Jul 16;48(10):1944-9.
- Loeser RF, Goldring SR, Scanzello CR, Goldring MB. Osteoarthritis: a disease of the joint as an organ. *Arthritis Rheum*. 2012 Jun;64(6):1697-707.
- Rapp AE, Bindl R, Recknagel S, Erbacher A, Müller I, Schrezenmeier H, Ehrthaller C, Gebhard F, Ignatius A. Fracture healing is delayed in immunodeficient NOD/scid-IL2Rγnull mice. *PLoS One*. 2016 Feb 5;11(2):e0147465.
- Cai X, Wong YF, Zhou H, Xie Y, Liu ZQ, Jiang ZH, Bian ZX, Xu HX, Liu L. The comparative study of Sprague-Dawley and Lewis rats in adjuvant-induced arthritis. *Naunyn-Schmiedeberg's Arch Pharmacol*. 2006 May;373(2):140-7.
- Crosio G, Huang AH. Innate and adaptive immune system cells implicated in tendon healing and disease. *Eur Cell Mater*. 2022 Feb 18;43:39-52.
- Kimura T, Ozaki T, Fujita K, Yamashita A, Morioka M, Ozono K, Tsumaki N. Proposal of patient-specific growth plate cartilage xenograft model for FGFR3 chondrodysplasia. *Osteoarthritis Cartilage*. 2018 Nov;26(11):1551-61.